

# The *Entamoeba histolytica* EhPgp5 (MDR-like) Protein Induces Swelling of the Trophozoites and Alters Chloride-Dependent Currents in *Xenopus laevis* Oocytes

DULCE MARÍA DELGADILLO,<sup>1</sup> D. GUILLERMO PÉREZ,<sup>1</sup> CONSUELO GÓMEZ,<sup>1</sup> ARTURO PONCE,<sup>2</sup> FRANCISCO PAZ,<sup>1</sup> CECILIA BAÑUELOS,<sup>3</sup> LEOBARDO MENDOZA,<sup>1,3</sup> CÉSAR LÓPEZ,<sup>1</sup> and ESTHER OROZCO<sup>1,3</sup>

## ABSTRACT

*Entamoeba histolytica*, the protozoan responsible for human amoebiasis, presents the multidrug resistant phenotype due to the expression of the *E. histolytica* P-glycoproteins EhPgp1 and EhPgp5. Here, we studied the protein EhPgp5 encoded by the *EhPgp5* gene in emetine-sensitive trophozoites transfected with the *pEhNEOPgp5* plasmid carrying the *EhPgp5* gene. The transfected trophozoites increased their drug resistance slightly, but became bigger and globular. To investigate other EhPgp5 functions further, we microinjected the *EhPgp5* mRNA in *Xenopus laevis* oocytes. Microinjected oocytes expressed EhPgp5 protein in their membranes and exhibited an ion current not present in the control oocytes. The antisense *EhPgp5AS* transcript, co-injected with the *EhPgp5* mRNA, abolished the exogenous current, showing its specificity. Exogenous current was outward during depolarizing pulses. Reduction of the extracellular Cl<sup>-</sup> concentration displayed a reversible decrease of the current amplitude. Niflumic acid, 4,4-diisothiocyanatostilbene-2, 2'-disulfonic acid, and other Cl<sup>-</sup> channel blockers abolished the exogenous current, which was poorly modified by verapamil and changes in osmolarity of the medium. Our results suggest that the EhPgp5 protein could function as a Cl<sup>-</sup> current inductor and as a coadjuvant factor to avoid drug accumulation in the cell.

## INTRODUCTION

*ENTAMOEBIA HISTOLYTICA*, the protozoan responsible for human amoebiasis, infects 500 million people, provokes 50 million cases of dysentery or liver abscesses, and kills 100,000 humans each year around the world.<sup>45</sup> Amoebiasis is controlled primarily by drug medication of symptomatic individuals, using mainly metronidazole and emetine. However, differences in drug susceptibility have been reported for *E. histolytica* isolates<sup>8,37</sup> and laboratory-cultured strains.<sup>31</sup> There are also case reports of failed drug treatments.<sup>21,35</sup> These results and the generation in the laboratory of multidrug-resistant (MDR) trophozoites (clone C2),<sup>31,34</sup> suggest that the parasite can develop the MDR phenotype in its human host.

P-glycoproteins (Pgps) encoded by the *mdr* genes are energy-dependent pumps and act as multidrug transporters in

MDR cells.<sup>15,24</sup> Pgps have been also involved in the stress response, in removing toxic substances from the cell, in cytokines transport, in lipid translocation, in apoptosis, and as regulators of the volume-activated chloride (Cl<sup>-</sup>) channels.<sup>26</sup> Transfection of the human *MDR1* cDNA into mammalian cells caused the appearance of a swelling-activated Cl<sup>-</sup> conductance.<sup>2,41</sup> It has been reported that simultaneous anion conductance and pump activity cannot occur. Reversible phosphorylation has been suggested as a possible event for regulating the drug transport and Cl<sup>-</sup> channel functions.<sup>25</sup> It has been proposed that the Pgp encoded by the human *MDR1* gene does not have intrinsic channel activity,<sup>43</sup> but regulates other endogenous Cl<sup>-</sup> channels.<sup>6,23,29</sup>

In *E. histolytica*, the drug-resistant trophozoites of clone C2 show a poor drug accumulation in their cytoplasm.<sup>33</sup> Their multidrug resistance is reversed by verapamil to the level exhibited by the drug-sensitive trophozoites of the clone A.<sup>31</sup> At least

<sup>1</sup>Program of Molecular Biomedicine, CICATA IPN, Col. Irrigación, México 11500, D.F.  
Departments of <sup>2</sup>Physiology, Biophysics and Neurosciences and <sup>3</sup>Experimental Pathology, CINVESTAV IPN, A.P. 14-740, México 07000, D.F.

four different *E. histolytica* Pgps (*EhPgps*) *mdr*-like genes (*EhPgp1*, *EhPgp2*, *EhPgp5*, and *EhPgp6*) exist in this parasite,<sup>10,11</sup> but only the expression of the *EhPgp1* and *EhPgp5* genes correlates with drug resistance level in the trophozoites. The *EhPgp1* gene is constitutively overexpressed in drug-resistant trophozoites, whereas the *EhPgp5* gene is over-transcribed in the presence of emetine and the amount of transcript is augmented when drug concentrations are increased.<sup>11,32</sup> The *EhPgp1* and *EhPgp5* proteins are overexpressed in drug-resistant mutants, strongly suggesting that these products participate in the MDR phenotype of the parasite.<sup>5</sup> However, the contribution of each *EhPgp* gene to the MDR phenotype and other biological mechanisms in *E. histolytica* is unknown. By analogy with other Pgps, in addition to producing drug resistance in the trophozoites, the *EhPgps* could have an active role in ion conductance. Here, we investigated the function of the *EhPgp5* gene product (*EhPgp5*) in trophozoites transfected with the *pEhNEOPgp5* plasmid and in *Xenopus laevis* oocytes microinjected with the *in vitro*-transcribed *EhPgp5* mRNA.

## MATERIALS AND METHODS

### *E. histolytica* cultures

Trophozoites of clones A and C2 (strain HM1:IMSS)<sup>31</sup> were axenically cultured in TYI-S-33 medium, as described.<sup>12</sup>

### Cloning of the *EhPgp5* gene

The complete open reading frame (ORF) of the *EhPgp5* gene was cloned from the p12 and p4 recombinant pBluescript plasmids (pBS) (Stratagene, CA), obtained from a  $\lambda$  Zap II *E. histolytica* genomic DNA library.<sup>10</sup> The p12 plasmid contains 3,203 bp at the 5' end, whereas the p4 plasmid has 1,466 bp at the 3' end of the *EhPgp5* gene. Sense *EhPgp5*S25 (5'-TTGGT-ACCATGACAAGTGAACCAGC-3') and *EhPgp5*S19 (5'-GTTTCAGATATCCAACAAG-3') and antisense *EhPgp5*AS19 (5'-CTTGTTGGATATCTGAAAC-3') and *EhPgp5*AS25 (5'-AAGGATCCTTAATTCACAGTTCCAA-3') oligonucleotides were used to amplify by PCR the 3,190- and 716-bp fragments from the p12 and p4 plasmids, respectively. PCR-amplified fragments were joined by their unique *EcoRV* restriction site at base pair 3,190. The complete *EhPgp5* ORF was cloned in the transfection vector *pEhNEOCAT*<sup>22</sup> (kindly given by Dr. E. Tannich, Hamburg, Germany) by replacing the chloramfenicol acetyl transferase (*CAT*) gene by the *EhPgp5* gene into the *Kpn I/Bam HI* sites generating the *pEhNEOPgp5* plasmid. The *EhPgp5* ORF was also cloned in the transcription vector pBS-KS under the T7 promoter direction (*pBSEhPgp5*). To obtain the antisense *EhPgp5* transcript (*EhPgp5AS*), the *EhPgp5* gene was excised from the *pBSEhPgp5* plasmid and cloned into the pBS-SK vector, also under the T7 promoter but in the opposite direction, using the *Kpn I* and *Bam HI* enzymes. Sequences of constructions were analyzed by the dideoxynucleotide chain-termination method<sup>38</sup> using Sequenase version 2.0 DNA polymerase (U.S. Biochemical Corp).

### Transfection experiments

Trophozoites of clone A (10<sup>6</sup>) were transfected with 100  $\mu$ g of the *pEhNEOPgp5* or *pEhNEO* plasmids.<sup>30</sup> Electroporated

trophozoites were incubated in TYI-S-33 medium for 48 hr at 37°C. Cultures were supplemented first with 10 mg/ml and then with 50 mg/ml of G418 (Gibco/BRL). Growth curves were done starting with  $2 \times 10^5$  trophozoites cultured in the presence of 0, 20, and 40  $\mu$ M emetine. Cell number was evaluated every 24 hr. Trophozoites cultured on coverslips in the presence of 50 mg/ml of G418 were fixed with 3.7% paraformaldehyde and observed through an inverted microscope (Nikon) attached to a laser confocal system (MRC-1024, Bio Rad, CA). Cell volume was directly measured through the microscope using public domain software.

### RT-PCR assays

RNA was extracted from the trophozoites by the Trizol reagent (Gibco) and incubated for 15 min at 37°C with 10 U of RNase-free DNase I (Stratagene). Single-stranded cDNAs were synthesized using 200 U of Superscript II reverse transcriptase (Gibco) and oligo(dT). Multiplex PCR was performed with 1/10 volume of the reverse transcription mixture, and 2.5 U *Taq* DNA polymerase, and the sense (*EhPgp5*, 5'-GTAGGAGGTGCAGTATTTCC-3', and *actin*, 5'-AGCTGTCTTTTCATTATATGC-3') and the antisense (*EhPgp5*, 5'-CCATCCTATTTCTTGTTGAC-3', and *actin*, 5'-TTCTCTTTCAGCAGTAGTGGT-3') oligonucleotides.<sup>11,14</sup> PCR was done in 22 cycles at 90°C for 30 sec; 52°C for 35 sec; 70°C for 90 sec. The products were analyzed in 12% polyacrylamide gel electrophoresis (PAGE).

### In vitro mRNA synthesis

The *pBSEhPgp5* and *pBSEhPgp5AS* plasmids were linearized with *Sac I* and *Kpn I* enzymes, respectively. RNA synthesis was performed using a commercial kit (MAXiScript™, Ambion, TX), 0.5 mM each of ribonucleotides ATP, CTP, GTP, and UTP, 2  $\mu$ g of linearized plasmid DNA, 10 U of ribonuclease inhibitor, 2 mM of 5' cap analogue, and 20 U of T7 RNA polymerase. The mixture was incubated at 4°C for 16 hr. A 2- $\mu$ l aliquot was treated with 1 U of DNase I (RNase free) (Ambion) or with 40 ng of RNase A and 125 U of RNase T1 (RiboQuant, RPA Kit Pharmigen), for 45 min at 37°C. The capped mRNA concentration was spectrophotometrically determined. mRNA was ethanol precipitated and electrophoresed in 4% formaldehyde and 1.2% agarose gels.

### Isolation and microinjection of *X. laevis* oocytes

Oocytes from adult female *X. laevis* (*Xenopus 1*, Ann Arbor, MI) were prepared from anaesthetized frogs,<sup>29</sup> previously immersed in 0.17% cold tricaine (3-aminobenzoic acid ethyl ester methanesulphonate salt) (Sigma) for 5 min. Ovaries were surgically removed through a small incision in the lower abdomen and washed in OR2 solution (83 mM NaCl, 2.5 mM KCl, 1 mM CaCl<sub>2</sub>, 1 mM MgCl<sub>2</sub>, 5 mM HEPES, and 1 mM NaH<sub>2</sub>PO<sub>4</sub>, pH 7.6). Fully grown stage V and VI oocytes (1.2–1.3 mm diameter) were obtained by manual defolliculation and maintained in OR2 at 18°C until microinjection. Healthy oocytes were placed in a Petri dish fitted with a nylon cloth mesh (500  $\mu$ m) to be microinjected under a stereoscopic light microscope. We used a glass pipette with the tip mechanically broken to an outer diameter of 10–20  $\mu$ m, attached on a positive-displacement, variable-volume, 10- $\mu$ l nanoinjec-

tor (Microdispenser Digital VWR Scientific).<sup>13</sup> Then, 50 nl (1 ng/nl) of the *EhPgp5* or the *EhPgp5* and *EhPgp5AS* transcripts together or CAT mRNA transcript (used as a control), pBS DNA, or water were microinjected by impaling the animal hemisphere. Injected oocytes were maintained in ND96 solution (96 mM NaCl, 2 mM KCl, 1.8 mM CaCl<sub>2</sub>, 1 mM MgCl<sub>2</sub>, 10 mM HEPES, pH 7.5) supplemented with 2.5 mM sodium pyruvate and 100 μg/ml gentamicin (Gibco) at 18°C. The solution was changed daily.

#### *Immunofluorescence laser confocal microscopy experiments*

Oocytes were fixed for 4 hr with 3.7% formaldehyde, 0.25% glutaraldehyde, and 0.2% Triton X-100 in BRB buffer (80 mM PIPES, pH 6.8, 5 mM EGTA, 1 mM MgCl<sub>2</sub>). Then, they were incubated in methanol at -20°C overnight, rehydrated in phosphate-buffered saline (PBS) (130 mM NaCl, 2 mM KCl, 8 mM Na<sub>2</sub>HPO<sub>4</sub>, 1 mM K<sub>2</sub>HPO<sub>4</sub>, pH 6.8), and incubated for 16 hr at room temperature in PBS containing 100 mM NaBH<sub>4</sub>. Oocytes were extensively rinsed in Tris-buffered saline (TBS) (155 mM NaCl, 10 mM Tris-HCl, pH 7.4, 0.1% NP-40), rehydrated, and bisected using a fine scalpel blade, prior to processing for immunofluorescence.<sup>17</sup> Cells were incubated at 4°C for 24 hr with a rabbit antibody against the EhPgp384 recombinant peptide carrying a common sequence of the *EhPgps* genes<sup>5</sup> (1:100 in TBS, 0.5% BSA) and 24 hr with a fluorescein-conjugated goat anti-rabbit immunoglobulin G (IgG) (Zymed, CA) (1:50 in TBS/BSA). The oocytes were dehydrated, cleared in xylol, mounted in 0.5-mm well slides with No. 1 coverslips, and examined using the laser confocal microscope.

#### *Protein extraction and Western blot analysis*

The oocytes were washed with ND96, homogenized at 4°C in 10 μl of a solution containing 50 mM Tris-HCl pH 8.0, 300 mM sucrose, 0.5 mM phenylmethylsulfonyl fluoride (PMSF), and aprotinin, pepstatin A, and leupeptin (Sigma) at 5 μg/ml each. Samples were centrifuged at 11,000 × g for 15 min. The interfaces were centrifuged for 30 min at 30,000 × g. The pellets containing the oocytes membranes<sup>27</sup> were resuspended in 50 mM Tris-HCl pH 8.0, 0.5 mM PMSF, and 0.05% Triton X-100. Proteins were acetone-precipitated overnight at -20°C. The trophozoite proteins were prepared by freeze-thawing the cells in 100 mM *p*-hydroxymercuribenzoic acid (PHMB).<sup>16</sup> Then, 30 μg of proteins were electrophoresed on 7.5% sodium dodecyl sulfate (SDS)-PAGE and transferred to nitrocellulose membranes (Amersham) for Western blot assay.<sup>39</sup> The EhPgp5 was detected using rabbit polyclonal antibodies against the EhPgp384 polypeptide (1:500) and anti-rabbit secondary IgG antibodies (1:1,000). Antigen-antibody reactions were revealed using the ECL kit (Amersham).

#### *Electrophysiological measurements*

Ion current measurements in the oocytes were made using a two-microelectrode voltage-clamp technique. The pipettes were pulled with a vertical pipette puller (David Kopf, Instruments, CA). Pipettes had resistances of 0.5–2.0 MΩ and were filled with 3 M KCl. Data were collected using a TEV-200 voltage clamp amplifier (Dagan Corporation, MP) attached to a Packard Bell microcomputer via a Digidata-1200 interface (Axon In-

struments Inc., CA) that was used to generate the voltage pulse protocols and to collect and analyze the currents. Current signals were filtered through a low-pass, 200-Hz Bessel filter and were acquired and analyzed with the pCLAMP software (version 6; Axon Instruments Inc.). Agar bridges (2% agarose in 3 M KCl) were connected to the bath to minimize junction potentials (less than 2 mV). Cells were transferred to the voltage-clamp chamber, which was continuously perfused at 0.5 ml/min with ND96 solution without sodium pyruvate and gentamicin. Oocytes were impaled and used only if they were in healthy conditions.

#### *Electrophysiological characterization of microinjected oocytes ion currents*

Cl<sup>-</sup> dependence of ion currents in the oocytes was tested by replacing the Cl<sup>-</sup> ions of the external solution by the impermeant anion methanesulfonate (MTS). Currents were recorded in oocytes bathed with ND96, ND81 (76 mM NaCl, 20 mM NaOH, 20 mM MTS, 2 mM KCl, 1.8 mM CaCl<sub>2</sub>, 2 mM MgCl<sub>2</sub>, 10 mM HEPES pH 7.5) or ND55 (50 mM NaCl, 46 mM NaOH, 46 mM MTS, 2 mM KCl, 1.8 mM CaCl<sub>2</sub>, 1 mM MgCl<sub>2</sub>, 10 mM HEPES pH 7.5) solutions. In some experiments 4,4-dithiocyanatostibene-2,2'-disulfonic acid (DIDS) (1 mM), niflumic acid (0.5 mM), 5-nitro-2-(3-phenylpropylamino) benzoic acid (NPPB) (500 μM) (Sigma), or 10 μM, 50 μM, and 1 mM verapamil were added to the bathing medium. The effect of osmolarity on ion currents was measured in ND50 (50 mM NaCl, 2 mM KCl, 1.8 mM CaCl<sub>2</sub>, 1 mM MgCl<sub>2</sub>, 10 mM HEPES pH 7.5) and ND50-sucrose (ND50 plus 100 mM sucrose). Experiments were performed at 22–25°C. The voltage-clamp protocol applied to the oocytes used a holding potential ( $E_h$ ) of -60 mV. The membrane potential of the oocyte was stepped with a series of pulses to -80 mV up to +80 mV (in 20-mV increments) lasting 800 msec. Data were sampled at 250 Hz.

Oocytes from the same frog were microinjected at the same time and divided in two groups. One was used for protein detection and the other for the electrophysiological studies. All experiments were performed at least five independent times using different oocyte batches.

#### *Statistics*

Each set of data was expressed as a mean ± SEM. Student's *t*-test was used to determine the statistical difference significance with  $p \leq 0.050$ .

## RESULTS

#### *Transfection of emetine-sensitive trophozoites with the pEhNEOPgp5 plasmid*

To initiate the study of the role of the EhPgp5 protein in the MDR phenotype, the full-length *EhPgp5* gene was cloned into the plasmid *pEhNEOPgp5* (Fig. 1A) and transfected into the emetine-sensitive trophozoites of clone A. The trophozoites transfected with the *pEhNEOPgp5* (AneoPgp5) augmented their drug resistance slightly; they died in 40 μM emetine (Fig. 1B). As expected, the trophozoite's transfected with the *pEhNEO*

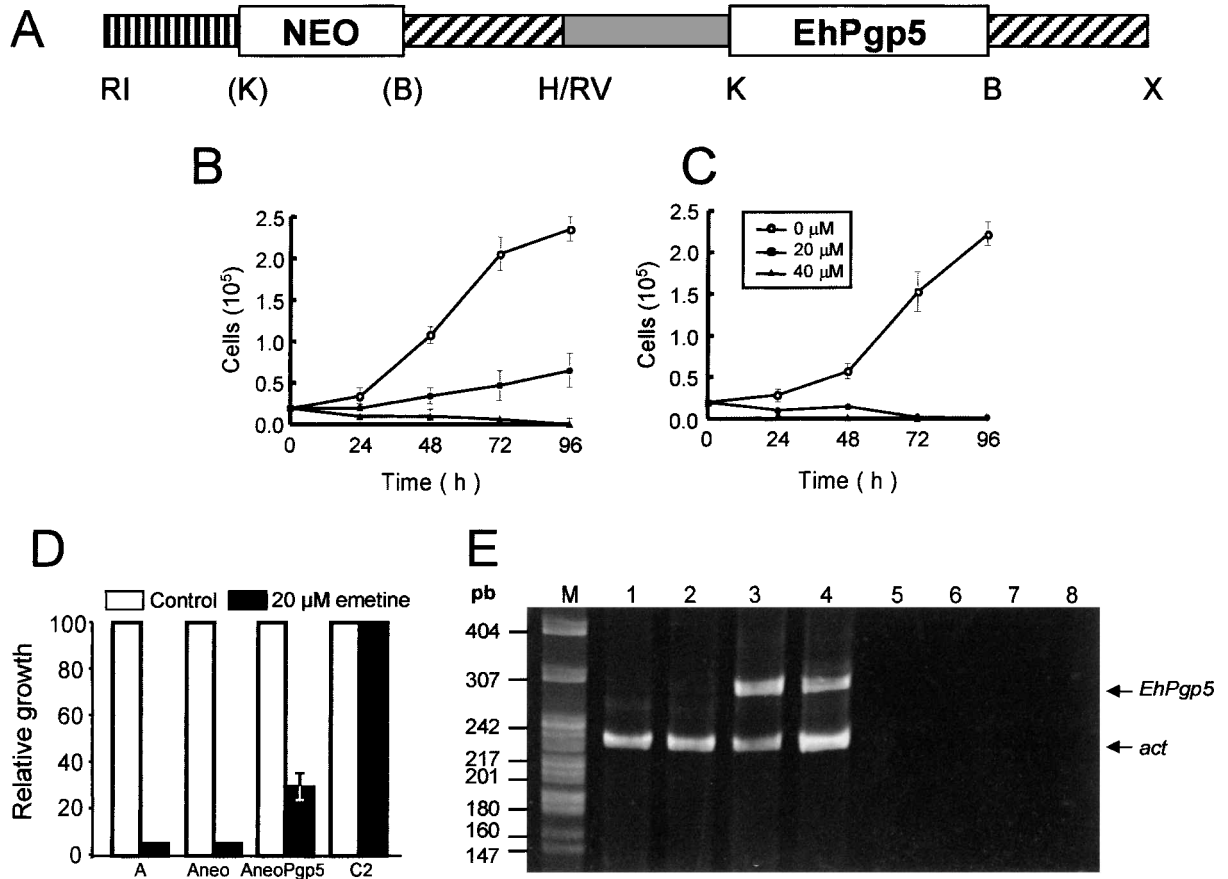


**FIG. 1.** Drug resistance and detection of the EhPgp5 and EhPgp1 genes in transfected trophozoites. **(A)** Scheme of *pEhNEOPgp5* plasmid used to transfect clone A trophozoites (AneoPgp5). *NEO*, Neomycin gene, flanked by 480 and 600 bp of the 5' (▨) and 3' (▩) untranslated sequences of the *E. histolytica actin* gene. EhPgp5, EhPgp5 full-length gene flanked by 485 bp of the 5' untranslated sequence (▧) of the *E. histolytica* 170-kDa lectin and 600 bp of the 3' untranslated sequence (▨) of the actin genes. RI, *Eco* RI; K, *Kpn* I, B, *Bam* HI, H, *Hind* III, RV, *Eco* RV, X, *Xba* I, restriction sites. **(B)** and **(C)** Growth curves in the presence of emetine: **(B)** AneoPgp5 trophozoites; **(C)** Aneo trophozoites. Symbols in the inset indicate the emetine concentration present in the culture medium. **(D)** Relative growth of trophozoites of clones A, Aneo, AneoPgp5, and C2. **(E)** RT-PCR of the *EhPgp5* gene in clone A trophozoites (lane 1), Aneo trophozoites (lane 2), AneoPgp5 trophozoites (lane 3), and clone C2 trophozoites (lane 4). *act*, Actin RT-PCR product obtained in the same reaction. Lanes 5–8 show the respective reaction mixture without RT.

plasmid (Aneo) did not augment their basal drug resistance (Fig. 1C,D). To confirm that the *EhPgp5* gene was being expressed in the AneoPgp5 trophozoites, we used specific primers<sup>11</sup> to perform RT-PCR assays. The *EhPgp5* gene was transcribed in the AneoPgp5 and clone C2 trophozoites (Fig. 1E, lanes 3 and 4), but not in the trophozoites of clone A and Aneo (Fig. 1E, lanes 1 and 2). These results may indicate that the expression of the *EhPgp5* gene alone is not sufficient to confer high drug resistance and that other factors might be involved in the *E. histolytica* MDR phenotype.

Interestingly, the AneoPgp5 trophozoites augmented their cell volume, compared with the Aneo and C2 trophozoites (Fig. 1A–C). The mean volume of 100 trophozoites of the clone Aneo was  $1.86 \pm 0.4 \mu\text{m}^3$  ( $p = 0.050$ ), the trophozoites of clone C2 measured  $1.29 \pm 0.3 \mu\text{m}^3$  ( $p = 0.050$ ), whereas the AneoPgp5 trophozoites measured  $2.5 \pm 0.10 \mu\text{m}^3$  ( $p = 0.050$ ) (Fig. 2D). The swelling of the *EhPgp5*-transfected cells suggested a mod-

ification in the membrane permeability of the AneoPgp5 trophozoites.

#### *In vitro* transcription of the *EhPgp5* gene and expression of the *EhPgp5* protein in *X. laevis* oocytes

To investigate whether the *EhPgp5* gene product altered the ion flux in the cells, we selected the well-described *X. laevis* oocytes model.<sup>7,29</sup> The full-length gene (*EhPgp5*) and its anti-sense chain (*EhPgp5AS*) were cloned into the pBS-KS and pBS-SK plasmids, respectively (Fig. 3A). Then, the *EhPgp5* and *EhPgp5AS* were transcribed *in vitro* using the T7 RNA polymerase. On agarose gels, the full-length transcripts were detected as 3.9-kb bands (Fig. 3B, lanes 1, 3, 5, and 7). Another 6.8-kb band, given by the plasmid DNA, used as template, was also present in the gels (Fig. 3B, lanes 1 and 5). When mixtures were incubated with RNase, the transcript disappeared and

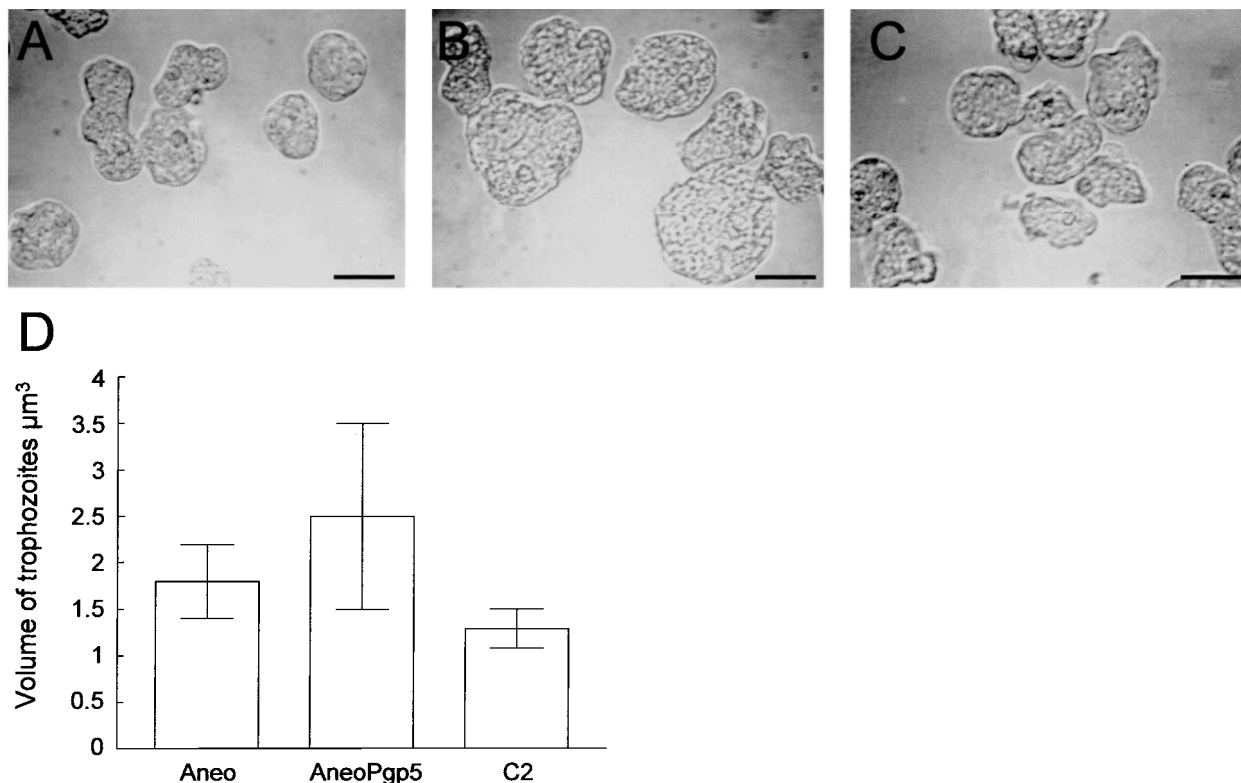


**FIG. 2.** Differences in the volume of the transfected trophozoites. Phase contrast of: (A) Aneo trophozoites; (B) AneoPgp5 trophozoites; (C) clone C2 trophozoites. Bar = 30  $\mu\text{m}$ . (D) Average of volume of 100 trophozoites shown in A, B, and C.

only the 6.8-kb DNA bands were detected (Fig. 3B, lanes 2 and 6). In contrast, when samples were treated with DNase, only the 3.9-kb transcripts were clearly visible (Fig. 3B, lanes 3 and 7). Incubation of the samples with both enzymes gave no bands (Fig. 3B, lanes 4 and 8). The DNase-treated *EhPgp5* mRNA was microinjected into the oocytes, and the EhPgp5 protein function was studied in these cells.

Confocal microscopy assays using the anti-EhPgp384 antibodies, directed against a EhPgp recombinant polypeptide, revealed a bright rim of fluorescence in the microinjected oocytes, showing the presence of EhPgp5 protein (Fig. 4A,B). We observed a fluorescent line in the outermost portion of the oocytes, corresponding to the cell membrane (Fig. 4A,B). Sections of the internal face of the oocytes exhibited a complex network of brightly stained material in the cytoplasm (Fig. 4B) where, according to Ward,<sup>44</sup> proteins are synthesized in the oocyte. A magnification of this material allowed to detect fluorescent vacuoles (Fig. 4C), by which newly synthesized proteins may be transported to the plasma membrane. No appreciable staining of the oocytes was seen when the primary antibody was omitted (Fig. 4D) or when nonmicroinjected oocytes were incubated with the primary and secondary antibodies (Fig. 4E).

Western blot assays of the oocyte membrane proteins using the anti-EhPgp384 antibodies showed the presence of a broad band, ranging between 144 and 184 kDa (Fig. 4F, lane 1). This molecular weight is in the expected range according to the 3.9-kb transcript injected into the oocytes. The broad range of the band may be due to the synthesis of different glycosylated forms

of EhPgp5 or to incomplete protein translation products. No bands were detected in proteins extracted from oocytes that were co-injected with the *EhPgp5* mRNA and its antisense *EhPgp5AS* transcript (Fig. 4F, lane 2), or in nonmicroinjected oocytes (Fig. 4F, lane 3) or in those injected with water or pBS DNA (data not shown). As expected, the antibody recognized a band of 147 kDa in proteins obtained from trophozoites of the drug-resistant clone C2, which over express the EhPgps (Fig. 4F, lane 4).

#### *Induction of ion currents in EhPgp5 mRNA-microinjected X. laevis oocytes*

Several studies have suggested that Pgps may act as  $\text{Cl}^-$  conductance proteins or as regulators of  $\text{Cl}^-$  conductance.<sup>40,41</sup> In *E. histolytica*, ion channels have not been studied yet, probably due to the technical difficulties related to perform patch clamp experiments in the trophozoites. To study the ion currents induced by *EhPgp5* mRNA, the microinjected oocytes were voltage-clamped and the membrane currents were recorded during step pulses following the protocol described in Materials and Methods and in Fig. 5A (inset). We analyzed the currents ( $I$ ) at +80 mV, under isotonic conditions every 24 hr after microinjection. Current values were measured at 200 msec from the start of the voltage pulse and plotted against the incubation time (Fig. 5A) ( $n = 15$  oocytes for each point). After 24 hr of incubation, the microinjected and the nonmicroinjected oocytes presented ion currents of similar amplitude ( $0.8 \pm 0.2$

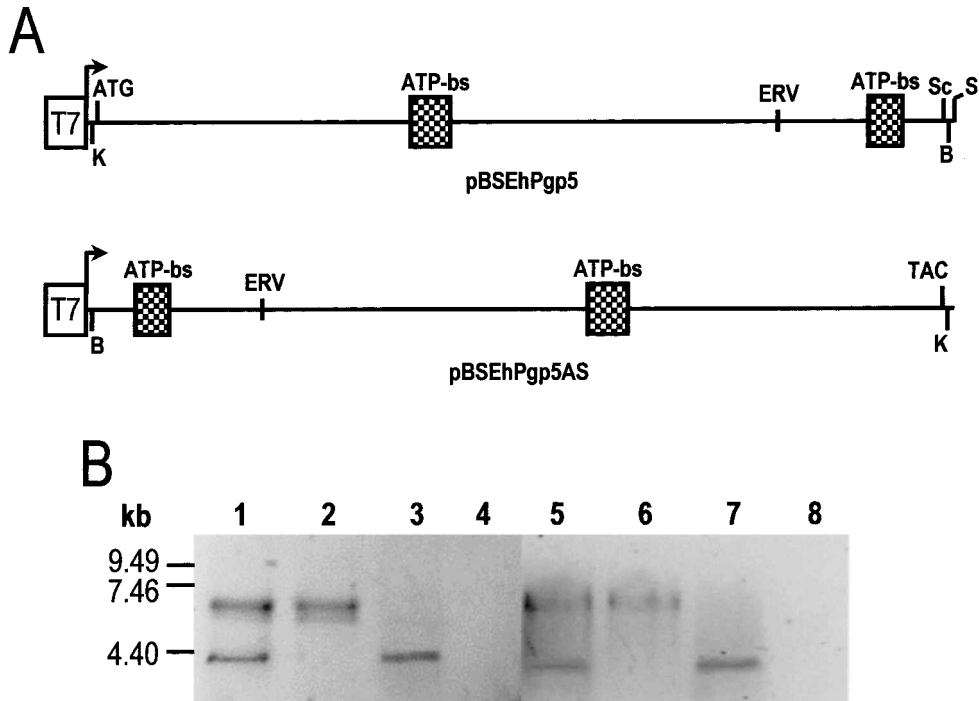


**FIG. 3.** Physical map of *EhPgp5* and *EhPgp5AS* DNA and their *in vitro* transcription products. **(A)** Scheme of *EhPgp5* gene and its *EhPgp5AS* antisense chain cloned into pBS-KS and pBS-SK, respectively. ATG, Translation initiation codon; ATP-bs, ATP-binding sites; TAC, complementary ATG sequence. Arrows indicate transcription initiation sites. ERV, *Eco* RV; K, *Kpn* I; B, *Bam* HI; S, *Sac* I restriction sites; Sc, stop codon; T7 box, T7 RNA polymerase promoter. **(B)** Ethidium bromide-stained agarose gel with the *in vitro* transcription products of the *EhPgp5* gene (lanes 1–4) and the *EhPgp5AS* antisense chain (lanes 5–8). The *in vitro* transcription products were treated with: none (lanes 1 and 5), RNase (lanes 2 and 6), DNase (lanes 3 and 7), RNase and DNase (lanes 4 and 8).

$\mu\text{A}$ ). However, at 48 hr, the membrane current increased in the microinjected oocytes to  $2.3 \pm 0.14 \mu\text{A}$ , at 72 hr to  $2.4 \pm 0.095 \mu\text{A}$ , at 96 hr to  $4.0 \pm 0.5 \mu\text{A}$ , and at 120 hr post-injection to  $6.0 \pm 0.3 \mu\text{A}$ . The noninjected oocytes had currents ranging between  $0.8 \pm 0.07$  and  $1.3 \pm 0.4 \mu\text{A}$  (Fig. 5A), indicating an increase of 2.8–7.5 times in the *EhPgp5* mRNA-microinjected oocytes. We selected oocytes incubated for 96 hr after microinjection to characterize the currents, because at this time, the majority of the cells appeared healthy, whereas at 120 hr post-injection several oocytes showed some damage in their structure.

Depolarization induced a gradual increase in the amplitude of outward currents that depended on the size of the pulse. The current observed at +80 mV in *EhPgp5* mRNA-microinjected oocytes was  $4.1 \pm 1.7 \mu\text{A}$  ( $n = 38$ ). An example is illustrated in Fig. 5B. To prove that the ion currents were specifically due to the *EhPgp5* mRNA product, we injected the oocytes with 50 ng of each *EhPgp5* and the antisense *EhPgp5AS* transcripts. Similar to the traces shown in Fig. 5B, the currents obtained in these experiments with oocytes injected with the *EhPgp5* mRNA were  $4.1 \pm 0.6 \mu\text{A}$  (data not shown), whereas those of the co-injected oocytes averaged  $1.3 \pm 0.3 \mu\text{A}$ , as illustrated in Fig. 5C. Differences between the *EhPgp5*- and the *EhPgp5* plus *EhPgp5AS*-microinjected oocytes were statistically significant ( $p = 0.031$ ). Ion currents were abolished by the antisense transcript, strongly suggesting that currents were specifically given

by the *EhPgp5* gene expression. In contrast, the endogenous currents observed in noninjected, or pBS DNA-injected oocytes averaged  $1.8 \pm 0.2 \mu\text{A}$  ( $n = 38$ ). Figure 5D shows a representative experiment. An unrelated mRNA (50 ng) gave no ion currents (Fig. 5E). The current–voltage ( $I$ – $V$ ) relationship measured in the *EhPgp5* mRNA-microinjected oocytes was not linear and showed an outward rectifying behavior. Figure 5F is a plot of the amplitude of the currents as a function of the membrane potential of the experiment illustrated in Fig. 5B.

#### Detection of chloride-activated currents in *EhPgp5* mRNA-injected oocytes

To investigate the involvement of  $\text{Cl}^-$  ions in the currents transported through *EhPgp5* or to an *EhPgp5*-associated ion channel, we replaced part of the  $\text{Cl}^-$  ions by MTS in the bathing medium. In the experiment illustrated in Fig. 6A, the amplitude of the currents measured at +80 mV in ND96 solution (103 mM  $\text{Cl}^-$ ) was taken as 100%. In ND81 solution (81 mM  $\text{Cl}^-$ ), the amplitude was 53% and in ND55 solution (55 mM  $\text{Cl}^-$ ), it dropped to 43% (Fig. 6A). Although the amplitude of the currents in 103 mM  $\text{Cl}^-$  varied among the different experiments performed (from 4.1 to 4.5  $\mu\text{A}$ ), the replacement of  $\text{Cl}^-$  by MTS reproducibly reduced their amplitude. We also observed in the corresponding current–voltage relationships for each solution, a shift in the reversal potential to positive values. These

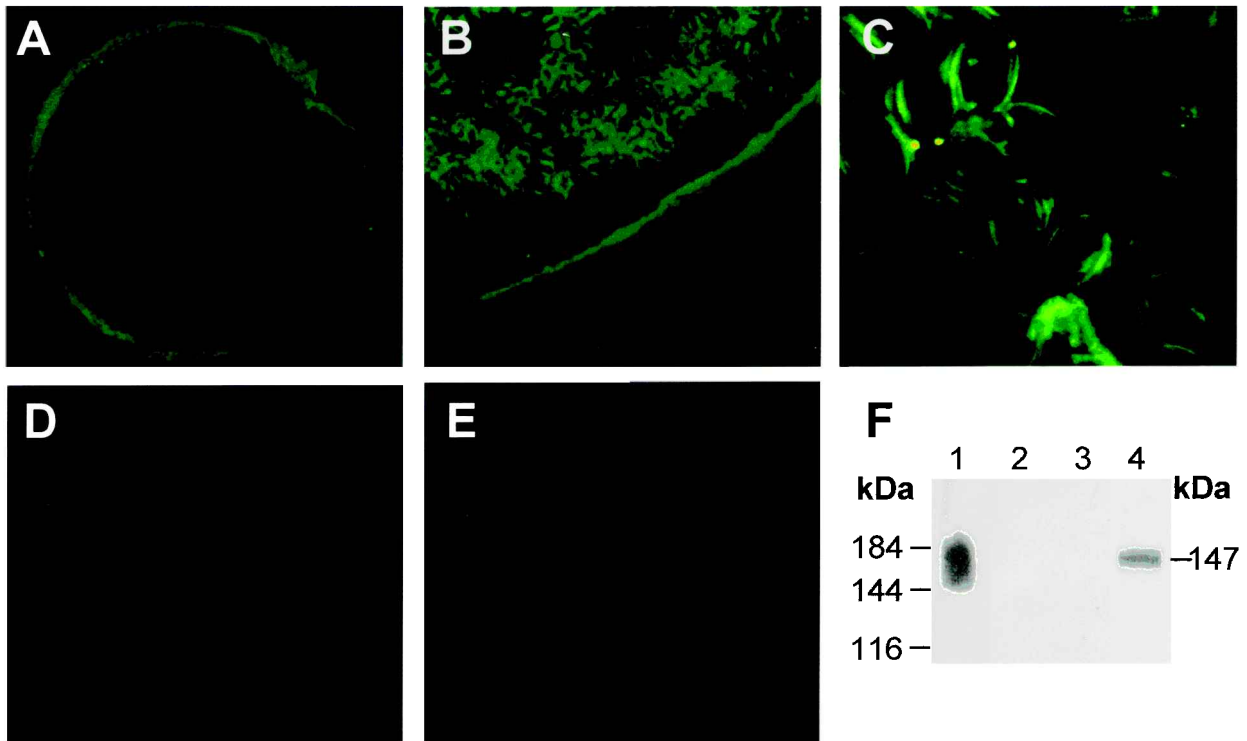


**FIG. 4.** Confocal microscopy and Western blot of EhPgp5 in *X. laevis* oocytes. *EhPgp5* mRNA-microinjected oocytes were fixed, hemisected, and incubated with the anti-EhPgp384 antibody and then, with an anti-FITC-labeled goat anti-rabbit IgG secondary antibody. (A–C) Different sections of a hemisected oocytes. Magnifications: (A) 10 $\times$ , (B) 40 $\times$ , (C) 100 $\times$ . (D) *EhPgp5* mRNA-microinjected oocyte incubated only with the secondary antibody. (E) Nonmicroinjected oocyte incubated with the primary and secondary antibodies. (F) Western blot of oocytes membrane proteins using the anti-EhPgp384 antibody. Oocytes were microinjected with: *EhPgp5* mRNA (lane 1), *EhPgp5* and *EhPgp5AS* transcripts (lane 2), and water (lane 3). Total proteins of clone C2 trophozoites (lane 4).

results support the view that  $\text{Cl}^-$  participates in the induced currents. The effect of  $\text{Cl}^-$  replacement was reversible in all experiments done ( $n = 4$ ) (Fig. 6A). The noninjected cells did not show any changes when  $\text{Cl}^-$  was replaced by MTS (data not shown).

To obtain further evidence on the  $\text{Cl}^-$  ion dependence of the currents presented by the *EhPgp5* mRNA-injected oocytes, we incubated the oocytes in solutions containing different  $\text{Cl}^-$  and  $\text{Ca}^{2+}$  transport blockers (Fig. 6B–D). In Fig. 6B and D, we display results from representative experiments done with DIDS (1 mM), which inhibited the current by 68%. We also used niflumic acid (500  $\mu\text{M}$ ) (Fig. 6D) and NPPB (500  $\mu\text{M}$ ) (Fig. 6D), which inhibited the current by 63% and 80%, respectively. After 10 min of washout, the oocytes incubated in DIDS fully recovered the ion current (Fig. 6B), whereas the effect produced by niflumic acid was reversed in 72% (data not shown). The electrophysiological recordings of the oocytes microinjected with the *EhPgp5* transcript and incubated in the presence of 10  $\mu\text{M}$ , 50  $\mu\text{M}$  (data not shown), and 1 mM verapamil indicated that this drug had a poor effect (20% inhibition at the highest concentration) on the induced currents (Fig. 6C,D). The effect of the  $\text{Ca}^{2+}$  channel blocker verapamil on the currents induced by EhPgp5 was tested because in NIH-3T3 fibroblast transfected with the *MDR* gene<sup>41</sup> and in drug-resistant mutants of *E. histolytica*<sup>4</sup> the drug resistance was reversed by 50 and 10  $\mu\text{M}$

verapamil, respectively. Figure 6D presents a summary of the inhibitory effect of  $\text{Cl}^-$  channels blockers and verapamil on the *EhPgp5*-induced current at +80 mV. The amplitude decrease of the ion currents by these  $\text{Cl}^-$  transport inhibitors supports the notion that the EhPgp5 function is related to a  $\text{Cl}^-$  channel activity in the microinjected oocytes.

#### Swelling response in *EhPgp5* mRNA-injected oocytes

The AneoPgp5 trophozoites presented a volume increase after transfection (Fig. 2). Additionally, the expression of the human Pgp in transfected NIH-3T3 cells has been associated with  $\text{Cl}^-$  currents activated by cell swelling.<sup>41</sup> However, in rat colon cancer cells, a direct correlation between Pgp expression, the increase of cell volume, and  $\text{Cl}^-$  currents was not found.<sup>9</sup> We studied the  $\text{Cl}^-$  ion currents expressed in the *EhPgp5* mRNA-microinjected oocytes, which were bathed with solutions having different osmolarity. It has been reported that manual defolliculated oocytes incubated for 96 hr in isotonic conditions do not express endogenous currents due to a volume increase.<sup>1</sup> Results shown in Fig. 7 evidenced that the nonmicroinjected oocytes did not present any endogenous currents, even in the presence of a hypotonic solution. In contrast, the *EhPgp5* mRNA-microinjected oocytes, incubated for 30 min in the hypotonic ND50 solution, presented a slightly current amplitude

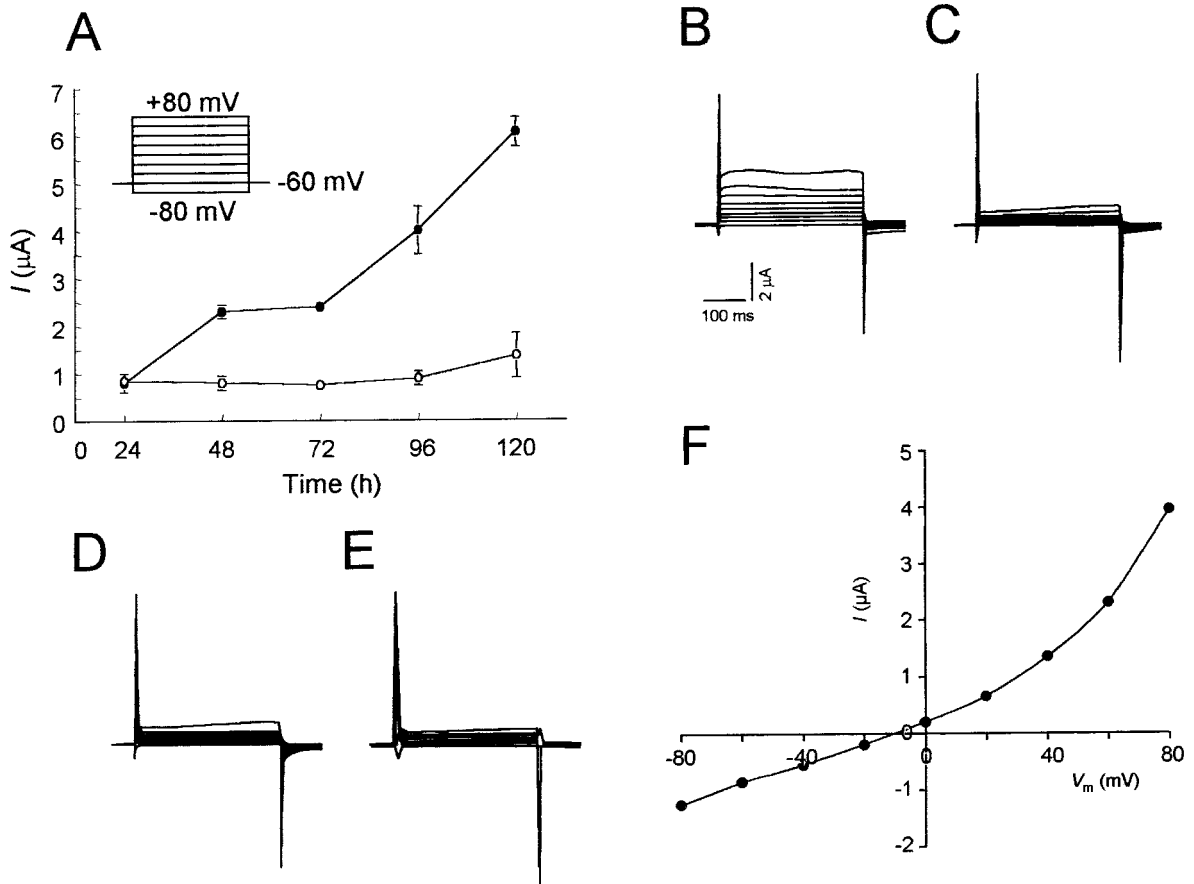


**FIG. 5.** Time-dependent expression and characterization of membrane currents in *X. laevis* oocytes microinjected with the *EhPgp5* mRNA. (A) Peak current values recorded at +80 mV measured in isotonic conditions (ND96 solution) at 24, 48, 72, 96 and 120 hr after microinjection. (●) Oocytes microinjected with *EhPgp5* mRNA; (○) oocytes microinjected with water. Data are expressed as the mean  $\pm$  SEM ( $n = 15$  oocytes per point). (Inset) Voltage protocol, the  $E_h$  was  $-60$  mV and the membrane potential of the oocyte was stepped to  $-80$  mV up to  $+80$  mV with steps of 20 mV. (B–E) Representative current traces recorded from *X. laevis* oocytes 4 days after microinjection with: (B) 50 ng (1 ng/ml) of *EhPgp5* mRNA ( $n = 38$  oocytes); (C) 50 ng of *EhPgp5* mRNA and 50 ng of *EhPgp5AS* transcript ( $n = 6$  oocytes); (D) 50 nl of water ( $n = 38$  oocytes); (E) 50 ng of CAT mRNA. (F) Current-voltage ( $I$ – $V$ ) relationship of the currents shown in B.

increased at all potentials. However, no statistical differences between these currents and those obtained in the microinjected oocytes perfused in isotonic solutions (ND50-sucrose) ( $n = 5$  oocytes per point) were found. The time course of activation, voltage dependence, magnitude of the current, and the reversal potential were not significantly altered when the osmolarity of the bathing solutions was changed.

## DISCUSSION

We have studied the function of the *EhPgp5* gene product in transfected trophozoites of *E. histolytica* and *EhPgp5* mRNA-microinjected *X. laevis* oocytes. Our results suggest that the EhPgps perform other functions in addition to contribute to the MDR phenotype. In the trophozoites, EhPgp5 produced swelling, suggesting that this protein could be involved in membrane permeability, probably functioning as a cell volume regulator. However, other causes for the volume

increase, such as *de novo* membrane synthesis, cannot be excluded.

Trophozoites transfected independently with the *EhPgp5* (Fig. 1B) or with the *EhPgp1* genes<sup>18</sup> reached a drug resistance level 10 times lower than the mutant clone C2 growing in 200  $\mu$ M emetine and expressing both genes.<sup>11,18</sup> Thus, the MDR phenotype exhibited by the drug-resistant trophozoites of the clone C2 might be given by a cooperative mechanism between the *EhPgp1* and the *EhPgp5* genes, but participation of other unidentified factors in this phenomenon is likely.

Our previous experiments have shown that trophozoites of clone A have the *EhPgp1* and *EhPgp5* genes, but *EhPgp5* is not transcribed and *EhPgp1* is poorly expressed.<sup>33</sup> After chemical mutagenesis of clone A, followed by the presence of emetine in the culture medium, we selected the clone C2, which grew in 20  $\mu$ M emetine and presented cross-resistance to other drugs.<sup>31</sup> Step selection of clone C2 in higher emetine concentrations generated trophozoites resistant up to 200  $\mu$ M emetine. They constitutively overtranscribed *EhPgp1*, but *EhPgp5* gene



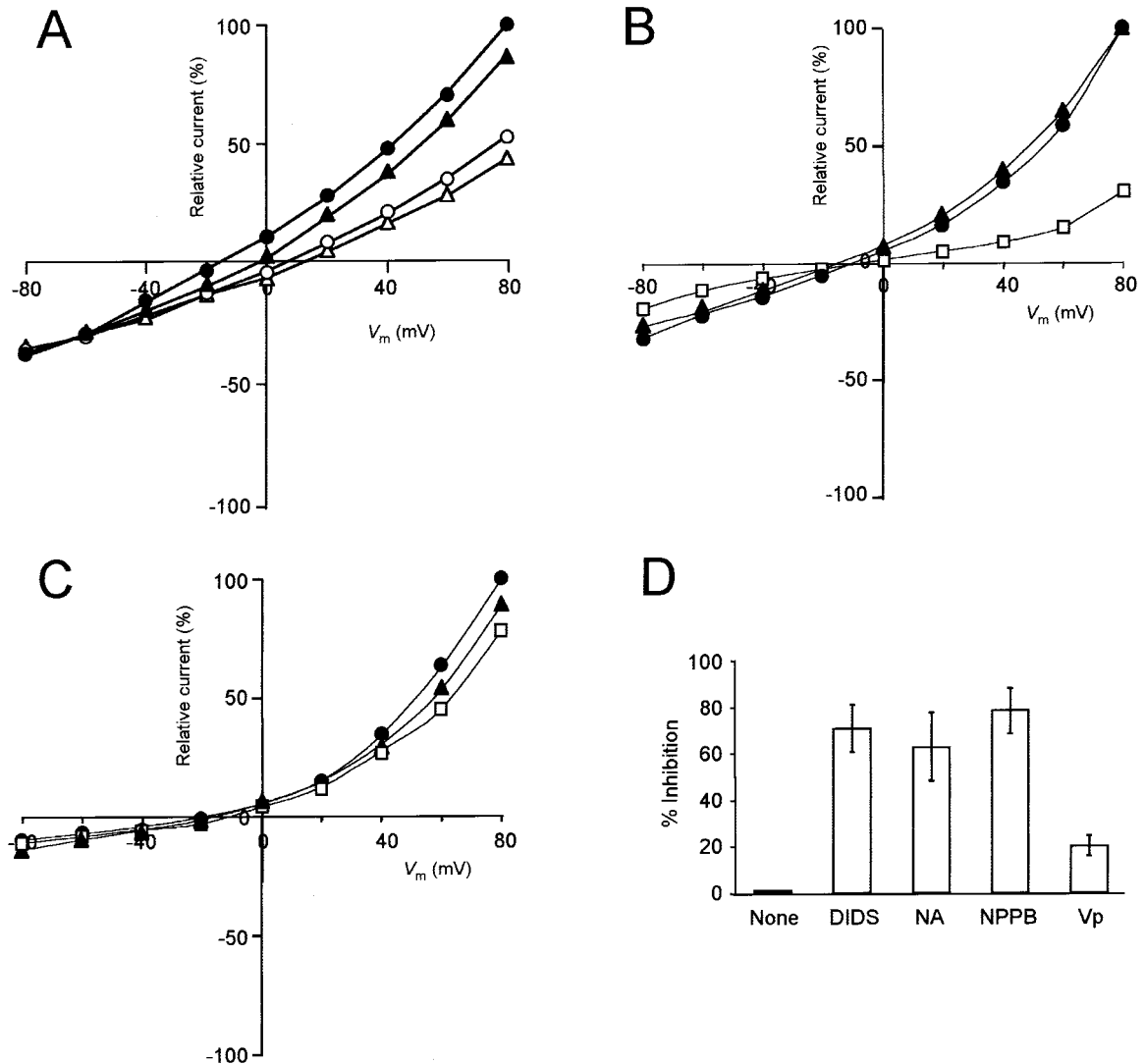


**FIG. 6.** Chloride dependence and effect of chloride channels blockers on *EhPgp5* mRNA-microinjected oocytes. **(A)** Representative *I-V* relationship of oocytes bathed with ND96 solution (●), ND81 solution (○), ND55 solution (△), ND96 washout of MTS (▲) ( $n = 4$ ). **(B and C)** *I-V* relationship from separate experiments in the presence of 1 mM DIDS **(B)** and 1 mM verapamil **(C)**. Bathing solutions were ND96 (●), ND96 plus inhibitor (□), and ND96 washout (▲) of the inhibitor. **(D)** Effect of Cl<sup>-</sup> channel blockers in the *EhPgp5* mRNA-microinjected oocytes at +80 mV. DIDS, 4,4-Diisothiocyanatostilbene-2,2'-disulfonic acid; NA, niflumic acid; NPPB, 5-nitro-2-(3-phenylpropylamino) benzoic acid; Vp, verapamil.

transcription was induced only when the drug was present in the medium. *EhPgp1* and *EhPgp5* gene promoters are identical in both clones. However, transfection of the trophozoites with the *EhPgp1* and *EhPgp5* promoters cloned in front of the *CAT* reporter gene, showed that *CAT* is poorly expressed in clone A, whereas it is abundantly expressed in clone C2.<sup>20,34</sup> These results indicate that other factors (some of them may be transcription factors) present in clone C2 are regulating the MDR phenotype.

Interestingly, in *X. laevis* oocytes, the product of the *EhPgp5* mRNA induced Cl<sup>-</sup>-dependent ion currents. Pgp is thought to participate in the mechanisms for regulatory volume decrease (RVD) in mammalian cells, through membrane permeability modifications.<sup>19,25</sup> The volume increase of AneoPgp5 tropho-

zoites suggests that changes in their membrane permeability and EhPgp5 could be participating in both functions: RVD and the low drug-resistance were augmented in AneoPgp5 trophozoites.

The *EhPgp5* mRNA-microinjected-oocytes generated an induced outward Cl<sup>-</sup>-dependent current. This was proved by replacing the Cl<sup>-</sup> ions in the bathing solution by MTS and by inhibition of the currents by Cl<sup>-</sup> channel blockers as DIDS, NPPB, and niflumic acid. The ion current induced by EhPgp5 in the oocytes was also poorly activated by hyposmotic shock, as it has been shown for other MDR cells.<sup>2,36,42</sup> Valverde *et al.*<sup>41</sup> proposed that cells exposed to a hyposmotic bath produce sizeable inward and outward currents, suggesting the involvement of ion channels. The anionic nature of the Pgp-associated currents was confirmed by these authors by replacing the ex-

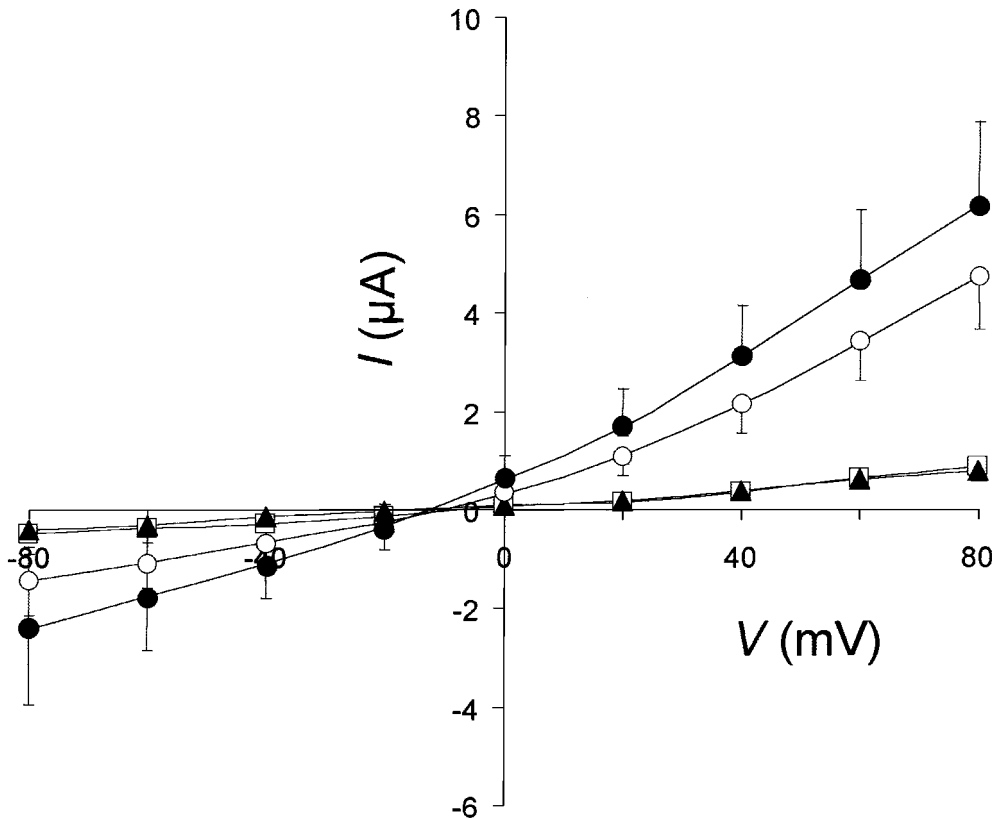


**FIG. 7.** Comparison of swelling-activated currents in *EhPgp5* mRNA-microinjected oocytes. Current–voltage ( $I$ – $V$ ) relationship of *EhPgp5* mRNA-microinjected oocytes exposed to isotonic (●) and hypotonic (○) solutions. (□) and (▲), Noninjected oocytes exposed to isotonic and hypotonic solutions, respectively. Each point represents the average of five experiments.

ternal  $\text{Cl}^-$  with gluconate, which largely decreases the outward current. Additionally, the current–voltage relation shows an outward rectification.

The ion current induced by EhPgp5 was poorly inhibited by verapamil. However, drug-resistance was reverted by verapamil in the trophozoites of the mutant clone C2. Our results suggest that verapamil may not have a strong and direct action on the EhPgp5. It could be acting on the EhPgp1 or another unidentified factor also involved in the *E. histolytica* MDR phenotype.

It is known that high levels of membrane protein expression in *Xenopus* oocytes may result in the induction of an endogenous hyperpolarization-activated current.<sup>3,40</sup> In the presence of  $\text{Ca}^{2+}$  ions, the current comprises two components, a  $\text{Ca}^{2+}$ -activated  $\text{Cl}^-$  current and a nonselective cation current. The  $\text{Cl}^-$  channel appears to be activated by  $\text{Ca}^{2+}$  flowing into the cell through nonselective channels.<sup>40</sup> These endogenous  $\text{Cl}^-$  currents become evident in the hyperpolarization range of membrane potentials at about  $-130$  mV.<sup>3</sup> Attali *et al.*<sup>3</sup> compared oocytes injected with different concentrations of *min K* mRNA at the same post-injection time and found that the hyperpolarization-activated  $\text{Cl}^-$  current was detected only when high mRNA concentrations were used. In the experiments shown here,  $\text{Cl}^-$  currents were activated during depolarization potentials and oocytes were injected with 50 ng of mRNA as Morin *et al.*<sup>29</sup> did in their studies on the *MDR1* human protein. Additionally, in parallel experiments, we injected in the oocytes 50

ng of a nonrelated mRNA (CAT mRNA), and no endogenous  $\text{Cl}^-$  currents were found in these experiments (Fig. 5E). Therefore, the contribution of endogenous  $\text{Cl}^-$  currents in our experiments is expected to be negligible. Additionally, the specificity of the ion current given by EhPgp5 in the oocytes was probed by blocking the translation of the *EhPgp5* mRNA with its antisense transcript.

In conclusion, our results show that the *EhPgp5* gene product might have a double function. It acts as a drug pump and could function also as a RVD in the trophozoites. The later mechanism could be associated with the  $\text{Cl}^-$  ion current induction present in the microinjected oocytes. Depending on the selection pressure, the trophozoites could express EhPgps able to perform one or another function. Here, we demonstrate that the frog oocytes are a suitable model to study the physiology of EhPgps, and that EhPgp5 exhibits properties that fit well with its participation in the flux of  $\text{Cl}^-$  ions as it has been proposed for other Pgps. However, we are aware that, due to the evolutionary distance between this protozoan and *X. laevis*, we cannot completely extrapolate the results obtained in the oocytes to the trophozoites.

EhPgp5 is one of the first channel-associated proteins cloned and functionally characterized in this parasite. The other one is the amebapore (AP), which produces damage to target cells through the membrane assembly of structural and functional pores.<sup>28</sup> AP does not exhibit any ion selectivity and is resistant to the effects of a transmembrane electric field.

Experiments in progress to define the role of several transcription factors on the expression of *EhPgp* genes will help us to understand better how they are regulated and what are the physiological relationships between the EhPgp1 and EhPgp5 proteins in the *E. histolytica* MDR phenotype. Additionally, the study of other functions performed by the EhPgp1 and EhPgp5 proteins will determine if they are involved in other functions already described for MDR proteins in Mammalia.

## ACKNOWLEDGMENTS

The authors wish to express their gratitude to Dr. Jorge A. Sánchez for critical reading and commenting upon the manuscript. Our thanks are also due to Alfredo Padilla for his help with the artwork. Dr. Orozco is an International Fellow of Howard Hughes Medical Institute. This work was also supported by CONACyT and CEGEPI-IPN (México).

## REFERENCES

- Ackerman, M.J., K.D. Wickman, and D.E. Clapham. 1994. Hypotonicity activates a native chloride current in *Xenopus* oocytes. *J. Gen. Physiol.* **103**:153–179.
- Altenberg, G., J.W. Deitmer, D.C. Glass, and L. Reuss. 1994. P-glycoprotein-associated Cl<sup>-</sup> currents are activated by cell swelling but do not contribute to cell volume regulation. *Cancer Res.* **54**:618–622.
- Attali, B., E. Guillemare, F. Lesage, E. Honoré, G. Romey, M. Lazdunski, and J. Barhanin. 1993. The protein IsK is a dual activator of K<sup>+</sup> and Cl<sup>-</sup> channels. *Nature* **365**:850–852.
- Ayala, P., J. Samuelson, D. Wirth, and E. Orozco. 1990. *Entamoeba histolytica*: physiology of multidrug resistance. *Exp. Parasitol.* **71**:169–175.
- Bañuelos, C., D.G. Pérez, C. Gómez, and E. Orozco. 2000. Expression and immunodetection of a P-glycoprotein in emetine-resistant trophozoites of *Entamoeba histolytica*. *Arch. Med. Res.* **31**:S288–S290.
- Bond, T.D., M.A. Valverde, and C.F. Higgins. 1998. Protein kinase C phosphorylation disengages human and mouse-1a P-glycoproteins from influencing the rate of activation of swelling-activated chloride currents. *J. Physiol.* **508**:333–340.
- Castillo, G., J.C. Vera, C.H. Yang, S.B. Horwitz, and O.M. Rosen. 1990. Functional expression of murine multidrug resistance in *Xenopus laevis* oocytes. *Proc. Natl. Acad. Sci. USA* **87**:4737–4741.
- Cedeño, J.R., and D.J. Krogstad. 1983. Susceptibility testing of *Entamoeba histolytica*. *J. Infect. Dis.* **148**:1090–1096.
- De Greef, C., S. van der Heyden, F. Viana, J. Eggermont, E.A. De Bruijn, L. Raeymaekers, G. Droogmans, and B. Nilius. 1995. Lack of correlation between mdr-1 expression and volume-activation of chloride-currents in rat colon cancer cells. *Pflugers Arch.* **430**:296–298.
- Descoteaux, S., P. Ayala, E. Orozco, and J. Samuelson. 1992. Primary sequences of two P-glycoprotein genes in *Entamoeba histolytica*. *Mol. Biochem. Parasitol.* **54**:201–212.
- Descoteaux, S., P. Ayala, J. Samuelson, and E. Orozco. 1995. Increase in mRNA of multiple *Ehpgp* genes encoding P-glycoprotein homologues in emetine-resistant *Entamoeba histolytica* parasites. *Gene* **164**:179–184.
- Diamond, L.S., D.R. Harlow, and C. Cunnick. 1978. A new medium for axenic cultivation of *Entamoeba histolytica* and other Entamoeba. *Trans. Royal Soc. Trop. Med. Hyg.* **72**:431–432.
- Douglash, J., P.B. Osborne, Y. Cai, M. Wilkinson, M.J. Christie, and J.P. Adelman. 1990. Characterization and functional expression of a rat genomic DNA clone encoding a lymphocyte potassium channel. *J. Immunol.* **144**:4841–4850.
- Edman, U., I. Meza, and N. Agabian. 1987. Genomic and cDNA actin sequences from a virulent strain of *Entamoeba histolytica*. *Proc. Natl. Acad. Sci. USA* **84**:3024–3028.
- Endicott, J.A., and V. Ling. 1989. The biochemistry of P-glycoprotein mediated multidrug resistance. *Annu. Rev. Biochem.* **58**:137–171.
- García-Rivera, G., M.A. Rodríguez, R. Ocadiz, M.C. Martínez-López, R. Arroyo, A. González-Robles, and E. Orozco. 1999. *Entamoeba histolytica*: a novel cysteine protease and adhesin from the 112 kDa surface protein. *Mol. Microbiol.* **33**:556–568.
- Gard, D.L. 1991. Organization, nucleation and acetylation of microtubules in *Xenopus laevis* oocytes: A study by confocal immunofluorescence microscopy. *Dev. Biol.* **143**:346–362.
- Ghosh, S.K., A. Lohia, A. Kumar, and J. Samuelson, J. 1996. Overexpression of P-glycoprotein gene 1 by transfected *Entamoeba histolytica* confers emetine-resistance. *Mol. Biol. Parasitol.* **82**:257–260.
- Gill, D.R., S.C. Hyde, C.F. Higgins, M.A. Valverde, G.M. Mintening, and F.V. Sepúlveda. 1992. Separation of drug transport and chloride channel functions of the human multidrug resistance P-glycoprotein. *Cell* **71**:23–32.
- Gómez, C., G. Pérez, E. López-Bayghen, and E. Orozco. 1998. Transcriptional analysis of the *EhPgp1* promoter of *Entamoeba histolytica* multidrug-resistant mutant. *J. Biol. Chem.* **273**:7277–7284.
- Hanna, R.M., M.H. Dahniya, S.S. Badr, and A. El-Betagy. 2000. Percutaneous catheter drainage in drug-resistant amoebic liver abscess. *Trop. Med. Int. Health.* **5**:578–581.
- Hamann, L., R. Nickel, and E. Tannich. 1995. Transfection and continuous expression of heterologous genes in the protozoan parasite *Entamoeba histolytica*. *Proc. Natl. Acad. Sci. USA* **92**:8975–8979.
- Hardy, S.P., H.R. Goodfellow, M.A. Valverde, D.R. Gill, F.V. Sepúlveda, and C.F. Higgins. 1995. Protein kinase C-mediated phosphorylation of the human multidrug resistance P-glycoprotein regulates cell volume-activated chloride channels. *EMBO J.* **14**:68–75.
- Higgins, C.F., and M.M. Gottesman. 1992. Is the multidrug transporter a flippase? *Trends Biol. Sci.* **17**:18–21.
- Idriss, H.T., Y.A. Hannun, E. Boulpaep, and S. Basavappa. 2000. Regulation of volume-activated chloride channels by P-glycoprotein: phosphorylation has the final say! *J. Physiol.* **524**:629–636.
- Johnstone, R.W., A.A. Ruefli, and M.J. Smyth. 2000. Multiple physiological functions for multidrug transporter P-glycoprotein? *Trends Biochem. Sci.* **25**:1–6.
- Kume, S., A. Muto, J. Aruga, T. Nakagawa, T. Michikawa, T. Furuichi, S. Nakade, H. Okano, and K. Mikoshiba. 1993. The *Xenopus* IP<sub>3</sub> receptor: structure, function, and localization in oocytes and eggs. *Cell* **73**:555–570.
- Leippe, M., J. Andra, R. Nickel, E. Tannich, and H.J. Muller-Eberhard. 1994. Amebapores, a family of membranolytic peptides from cytoplasmic granules of *Entamoeba histolytica*: isolation, primary structure, and pore formation in bacterial cytoplasmic membranes. *Mol. Microbiol.* **14**:895–904.
- Morin, X.K., T.D. Bond, T.W. Loo, D.M. Clarke, and C.E. Bear. 1995. Failure of P-glycoprotein (MDR1) expressed in *Xenopus* oocytes to produce swelling-activated chloride channel activity. *J. Physiol.* **486**:707–714.
- Nickel, R., and E. Tannich. 1994. Transfection and transient expression of chloramphenicol acetyltransferase gene in the proto-

- zoan parasite *Entamoeba histolytica*. Proc. Natl. Acad. Sci. USA **91**:7095–7098.
31. Orozco, E., F. Hernández, and M.A. Rodríguez. 1985. Isolation and characterization of *Entamoeba histolytica* mutants resistant to emetine. Mol. Biochem. Parasitol. **15**:49–59.
  32. Orozco, E., G. Pérez, M.C. Gómez, and P. Ayala. 1995. Multidrug resistance in *Entamoeba histolytica*. Parasitol. Today **11**:473–475.
  33. Orozco, E., C. Gómez, and D.G. Pérez. 1999. Physiology and molecular genetics of multidrug resistance in *Entamoeba histolytica*. Drug Resis. Up. **2**:188–197.
  34. Pérez, G., C. Gómez, E. López-Bayghen, E. Tannich, and E. Orozco. 1998. Transcriptional analysis of the *EhPgp5* promoter of *Entamoeba histolytica* multidrug-resistant mutant. J. Biol. Chem. **273**:7285–7292.
  35. Pittman, F.E., and J.C. Pittman. 1974. Amebic liver abscess following metronidazole therapy for amoebic colitis. Amer. J. Trop. Med. Hyg. **23**:146–150.
  36. Rasola, A., L.J.V. Galiotta, D.C. Gruener, and G. Romeo. 1994. Volume-sensitive chloride currents in four epithelial cell lines are not directly correlated to the expression of the MDR-1 gene. J. Biol. Chem. **269**:1432–1436.
  37. Samarawickrema, N.A., D.M. Brown, J.A. Upcroft, N. Thammapalerd, and P. Upcroft. 1997. Involvement of superoxide dismutase and pyruvate: ferredoxin oxidoreductase in mechanisms of metronidazole resistance in *Entamoeba histolytica*. J. Antimicrob. Chemother. **40**:833–840.
  38. Sanger, F., S. Nicklen, and A.R. Coulson. 1977. DNA sequencing with chain-terminating inhibitors. Proc. Natl. Acad. Sci. USA **74**:5463–5467.
  39. Towbin, H., T. Staehelin, and J. Gordon. 1979. Electrophoretic transfer of proteins from polyacrylamide gels to nitrocellulose sheets: Procedure and some applications. Proc. Natl. Acad. Sci. USA **76**:4350–4354.
  40. Tzounopoulos, T., J. Maylie, and J.P. Adelman. 1995. Induction of endogenous channels by high levels of heterologous membrane proteins in *Xenopus* oocytes. Biophys. J. **69**:904–908.
  41. Valverde, M.A., M. Díaz, F.V. Sépulveda, D.R. Gill, S.C. Hyde, and C.F. Higgins. 1992. Volume-regulated chloride channels associated with the human multidrug resistance P-glycoprotein. Nature **355**:830–833.
  42. Vanoye, C.G., G.A. Altenberg, and L. Reuss. 1997. P-glycoprotein is not a swelling-activated Cl<sup>-</sup> channel; possible role as a Cl<sup>-</sup> channel regulator. J. Physiol. **502**:249–258.
  43. Viana, F., K. Van Acker, C. De Greef, J. Eggermont, L. Raeymaekers, G. Droogmans, and B. Nilius. 1995. Drug-transport and volume-activated chloride channel functions in human erythrocyte cells: relation to expression level of P-glycoprotein. J. Memb. Biol. **145**:87–98.
  44. Ward, R.T. 1962. The origin of protein and fatty yolk in *Tana pipiens*. II. Electron microscopy and cytochemical observations of young and mature oocytes. J. Cell. Biol. **14**:309–341.
  45. World Health Organization. Weekly Epidemiological Record. 1997. **72**:97–100.

Address reprint requests to:

Dr. Esther Orozco

Department of Experimental Pathology

CINVESTAV IPN, A.P. 14-740

México 07000, D.F.

E-mail: Esther@mail.cinvestav.mx